Oncogene
https://doi.org/10.1038/s41388-020-1369-2

ARTICLE

SDCBP/MDA-9/syntenin phosphorylation by AURKA promotes esophageal squamous cell carcinoma progression through the EGFR-PI3K-Akt signaling pathway

Ruijuan Du[1,2] · Chuntian Huang[1,2] · Hanyong Chen[3] · Kangdong Liu[1,2,4,5] · Pu Xiang[6] · Ning Yao[2] · Lu Yang[2] · Liting Zhou[1,2] · Qiong Wu[1,2] · Yaqiu Zheng[2] · Mingxia Xin[2] · Zigang Dong[1,2,4,5] · Xiang Li[1,2,4,5]

Received: 18 December 2019 / Revised: 19 May 2020 / Accepted: 11 June 2020

Abstract

SDCBP is an adapter protein containing two tandem PDZ domains mediating cell adhesion. The role and underlying molecular mechanism of SDCBP in ESCC remain obscure. Here, we report that SDCBP is frequently overexpressed in ESCC tissues and cells compared to normal controls and that its overexpression is correlated with late clinical stage and predicts poor prognosis in ESCC patients. Functionally, high expression of SDCBP is positively related to ESCC progression both in vitro and in vivo. Furthermore, mechanistic studies show that SDCBP activates the EGFR-PI3K-Akt signaling pathway by binding to EGFR and preventing EGFR internalization. Moreover, we provide evidence that AURKA binds to SDCBP and phosphorylates it at the Ser131 and Thr200 sites to inhibit ubiquitination-mediated SDCBP degradation. More importantly, the sites at which AURKA phosphorylates SDCBP are crucial for the EGFR signaling-mediated oncogenic function of SDCBP. Taken together, we propose that SDCBP phosphorylation by AURKA prevents SDCBP degradation and promotes ESCC tumor growth through the EGFR-PI3K-Akt signaling pathway. Our findings unveil a new AURKA–SDCBP–EGFR axis that is involved in ESCC progression and provide a promising therapeutic target for ESCC treatment in the clinic.

Introduction

Esophageal cancer (EC) is one of the most predominant malignancies worldwide [1], ranking as the sixth most common cause of cancer-related death and the seventh most commonly diagnosed cancer [2]. Esophageal squamous cell carcinoma (ESCC), which accounts for ~90% of EC cases, is the most common type of esophageal carcinoma in Asian countries, especially in China [3]. Due to atypical symptoms in early stage and the lack of effective treatment targets, the 5-year survival rate of ESCC remains low [4]. Thus, it is vital to investigate the molecular and pathogenic mechanisms illuminating ESCC carcinogenesis.

Aurora A (AURKA) belongs to a family of serine/threonine kinases that are primarily involved in cell cycle processes, including centrosome duplication, separation, and maturation [5]. Clinical data show that overexpression and amplification of AURKA is observed in ESCC and that

These authors contributed equally: Ruijuan Du, Chuntian Huang

Supplementary information The online version of this article (https://doi.org/10.1038/s41388-020-1369-2) contains supplementary material, which is available to authorized users.

✉ Zigang Dong
dongzg@zzu.edu.cn

✉ Xiang Li
lixiang@zzu.edu.cn

[1] Department of Pathophysiology, School of Basic Medical Sciences, Zhengzhou University, Zhengzhou 450001 Henan, China

[2] China-US (Henan) Hormel Cancer Institute, No. 127, Dongming Road, Jinshui District, Zhengzhou 450008 Henan, China

[3] The Hormel Institute, University of Minnesota, Austin, MN 55912, USA

[4] The Collaborative Innovation Center of Henan Province for Cancer Chemoprevention, Zhengzhou, China

[5] State Key Laboratory of Esophageal Cancer Prevention and Treatment, Zhengzhou University, Zhengzhou, Henan, China

[6] Department of Hematology, Affiliated Cancer Hospital of Zhengzhou University & Henan Cancer Hospital, Zhengzhou 450008 Henan, China

Published online: 22 June 2020

overexpressed AURKA is related to malignant progression and poor prognosis of patients [6–8]. Overexpression of AURKA results in the malignant progression of ESCC by enhancing MMP-2 expression and activity, which can occur through p38 MAPK and Akt signaling pathways [9]. Although AURKA plays an important role in ESCC development, the specific substrate and underlying molecular mechanism in ESCC remain unclear.

Syndecan binding protein (SDCBP), also called melanoma differentiation associated protein-9 (MDA-9) and syntenin, is an adapter protein containing two tandem PDZ domains. In the physiological cellular state, SDCBP regulates various cellular activities, including exosome biogenesis [10], neuromodulation and synaptic development [11], cell adhesion [12], and immunoregulation [13]. In addition to maintaining normal cellular processes, SDCBP exhibits oncogenic properties in melanoma [14–16], breast cancer [17, 18], glioma [19, 20], head and neck cancer [21], urothelial cell carcinoma [22], and gastric cancer [17]. Functionally, SDCBP drives cancer cell proliferation, migration, invasion, and angiogenesis to facilitate tumorigenesis. Moreover, SDCBP helps to maintain protective autophagy and inhibit anoikis in glioma stem cells [23, 24]. As a scaffold protein, PDZ domains enable SDCBP to interact with different oncogenic partners, such as c-Src, IGF1R, EGFR, and Frizzled-7, mediating the activation of p38 MAPK, NF-κB, STAT3, PI3K-Akt signaling or the Wnt pathway in several types of cancer [22, 25–27]. The oncogenic potential of SDCBP and its essential roles in metastasis makes it an intriguing target for anticancer therapy. Recently, a small-molecule inhibitor that selectively binds to the PDZ1 domain of SDCBP is developed; this inhibitor attenuates the increase in glioblastoma cell invasion following radiation [28]. Furthermore, peptides targeting SDCBP can inhibit the progression of cancer cells [29]. These studies provide evidence supporting SDCBP as a potential target for cancer therapy. However, the function of SDCBP in ESCC remains to be further determined.

In the present study, we demonstrated for the first time that high expression of SDCBP predicted poor prognosis in ESCC and promoted ESCC progression in vitro and in vivo. SDCBP sustained EGFR membrane localization and promoted EGFR autophosphorylation, thus activating the EGFR/PI3K/Akt signaling pathway. Moreover, we found that AURKA can bind with the PDZ1 domain of SDCBP and directly phosphorylate SDCBP at Ser131 and Thr200 sites. Furthermore, phosphorylation of SDCBP by AURKA maintained SDCBP stability by inhibiting its ubiquitination, and SDCBP phosphorylation was also responsible for its oncogenic function. Taken together, our results indicated that SDCBP can promote ESCC progression and suggested that the AURKA–SDCBP–EGFR axis might be a novel target for the treatment of ESCC.

Results

Increased SDCBP expression predicts poor prognosis in ESCC patients

To determine the role of SDCBP in ESCC, we initially measured SDCBP expression in a human ESCC tissue array by immunohistochemistry staining. SDCBP expression was significantly higher in ESCC cancer tissues than in paired (Fig. 1a, b) or unpaired (Fig. 1c) adjacent normal tissues. In the public Gene Expression Profiling Interactive Analysis (GEPIA) database, SDCBP expression was also significantly higher in esophageal carcinoma than in normal controls (Fig. 1d). Furthermore, clinical association analysis revealed that SDCBP expression was significantly associated with the large tumor size (T stage), lymph node involvement (N stage), and advanced tumor-node-metastasis stage of ESCC (Fig. 1e; Table 1), and among patients of all stages, patients in stage IV had the highest level of SDCBP (Fig. 1e). Moreover, Kaplan–Meier analysis demonstrated that the ESCC patients with high SDCBP expression had a significantly shorter overall survival than those with low SDCBP expression (Fig. 1f). These findings indicate that SDCBP is a critical molecular marker and an informative prognostic factor in ESCC.

High expression of SDCBP correlates with AURKA expression in ESCC

Dysregulation of protein kinases is involved in various processes of carcinogenesis through modulating the function of target oncogenic proteins. From the GEPIA database, we observed a positive correlation between SDCBP and AURKA expression levels in esophageal carcinoma (Fig. 2a). We then analyzed the correlation between the expression levels of the two proteins in the ESCC tissue array. We found that ESCC tissues with high levels of SDCBP had increased expression of AURKA compared with that in tissues with low levels of SDCBP (Fig. S1). Spearman correlation analysis showed that SDCBP and AURKA expression was closely associated with each other ($R = 0.55$, $P < 0.001$, Fig. 2b). High AURKA expression was detected in 34 of 49 (69.4%) ESCC samples with high SDCBP expression but only in 15 of 50 (30%) ESCC samples with low SDCBP expression (Fig. 2c). Furthermore, ESCC patients with low expression of both SDCBP and AURKA tended to have better overall survival than those with high expression of SDCBP and AURKA (Fig. 2d). Finally, we evaluated the expression levels of these two proteins in ESCC cell lines. As shown in Fig. 2e, the Western blotting results showed significantly higher expression of SDCBP in 4 out of 6 ESCC cell lines and significantly higher expression of AURKA in 5 out of 6

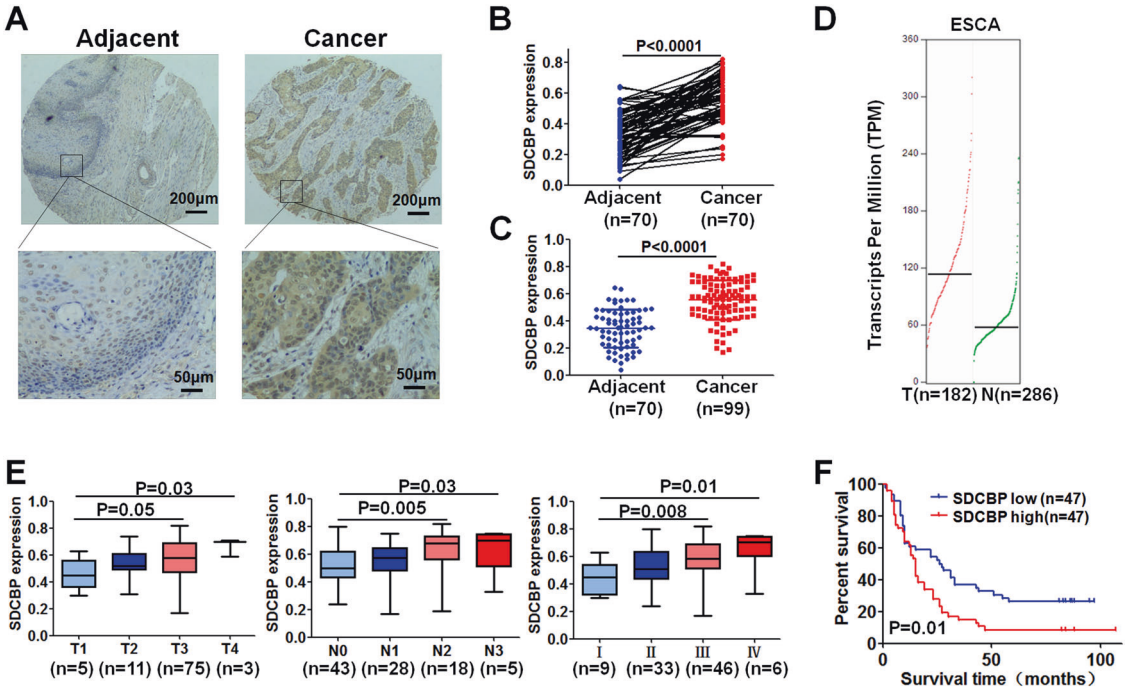

Fig. 1 Upregulated SDCBP predicts poor prognosis in ESCC patients. a Representative immunohistochemical staining images of a human ESCC tissue microarray using a specific antibody for SDCBP in adjacent tissues and paired cancer tissues. Statistical analysis was performed for immunohistochemical staining. SDCBP expression was valued as positivity. A summary of SDCBP expression is shown in paired (**b**) and unpaired (**c**) ESCC tissues. **d** SDCBP expression levels in normal or esophageal carcinoma tissues retrieved from the GEPIA database. **e** The expression levels of SDCBP in patients with different clinical stages from the ESCC tissue microarray. **f** Relationship between SDCBP expression levels and overall survival from an ESCC tissue microarray. Statistical analysis was performed using Student's paired *t* test in (**b**); Student's unpaired *t* test in (**c**, **e**); Kaplan–Meier analysis in (**f**). Error bars represent the mean ± SD.

ESCC cell lines. Spearman correlation analysis also indicated a similar expression pattern between SDCBP and AURKA in ESCC cell lines ($R = 0.96$, $P < 0.001$, Fig. 2f). Taken together, these data suggest that SDCBP and AURKA possess a close relationship with each other in ESCC.

SDCBP interacts with AURKA and is phosphorylated by AURKA

To explore the potential molecular mechanism between SDCBP and AURKA, immunoprecipitation assays were performed to check whether SDCBP can interact with AURKA. The results indicated that endogenous SDCBP can precipitate endogenous AURKA in KYSE410 cells and vice versa (Fig. 3a). Furthermore, an immunoprecipitation assay with ectopically expressed SDCBP and AURKA showed that His-tagged AURKA precipitated Flag-tagged SDCBP in transfected HEK293T cells (Fig. 3b).

To further determine whether the PDZ domains of SDCBP differentially contributed to the interaction with AURKA, we constructed a series of vectors with different SDCBP PDZ domain deletions (Fig. 3c). The immunoprecipitation results showed that AURKA precipitated WT-SDCBP, ΔPDZ2-SDCBP, and PDZ1 + PDZ2-SDCBP (Fig. 3d). These data suggested that the PDZ1 domain rather than the PDZ2 domain of SDCBP was essential for the association with AURKA. Moreover, the protein-docking model also showed that the PDZ domain of SDCBP can directly bind to AURKA's ATP binding pocket and then be phosphorylated by AURKA (Fig. 3e). Together, these data strongly suggest that SDCBP, especially the PDZ1 domain, can directly bind with AURKA.

As AURKA is a serine/threonine kinase and SDCBP interacts with AURKA, we next sought to demonstrate whether AURKA can phosphorylate SDCBP. An in vitro kinase assay showed that SDCBP can be directly phosphorylated by AURKA (Fig. 3f). Then we want to identify the potential sites of SDCBP that are phosphorylated by AURKA. We identified 12 possible SDCBP phosphorylation sites using the Netphos2.0 server (Fig. S2a). AURKA is a kinase that can recognize the consensus R/K/N-R-X-S/T-B, where B denotes any hydrophobic residue with the exception of Pro [30]. A hydrophobic residue at position $n + 1$ is a specificity determinant almost as powerful as the Arg–Arg doublet at positions $n - 2/n - 3$ [30]. Accordingly, there were three potential residues of SDCBP that might be phosphorylated by AURKA. To determine whether AURKA could phosphorylate these residues, we generated site mutants of SDCBP (S87A, S131A, and T200A),

Table 1 Correlation between SDCBP expression and clinicopathologic characteristics of ESCC.

Characteristics	SDCBP expression levels		
	Low ($n = 47$)	High ($n = 47$)	P
Gender			
Male	32 (68.1%)	38 (80.9%)	0.051
Female	15 (31.9%)	9 (19.1%)	
Age			
≤60	32 (68.1%)	31 (65.0%)	0.881
>60	15 (31.9%)	16 (34.0%)	
Histological grade			
Well/moderately	33 (70.2%)	34 (72.3%)	0.876
Poorly	14 (29.8%)	13 (27.7%)	
T classification			
T1	4 (8.5%)	1 (2.1%)	0.01
T2	7 (14.9%)	4 (8.5%)	
T3	36 (76.6%)	39 (83.0%)	
T4	0 (0.0%)	3 (6.4%)	
N classification			
N0	28 (59.6%)	15 (31.9%)	0.0002
N1	13 (27.7%)	15 (31.9%)	
N2	5 (10.6%)	13 (27.7%)	
N3	1 (2.1%)	4 (8.5%)	
Clinical stage			
I	7 (14.9%)	2 (4.3%)	<0.0001
II	21 (44.7%)	12 (25.2%)	
III	18 (38.3%)	28 (59.6%)	
IV	1 (2.1%)	5 (10.6%)	

and the in vitro kinase assay showed that S131 and T200 were likely the most important phosphorylation sites to be phosphorylated by AURKA (Figs. S2b, c and 3g). More notably, we analyzed the motif containing S131 and T200 in SDCBP in other species and found that the two sequences were highly evolutionarily conserved (Fig. 3h), suggesting that S131 and T200 are functionally relevant sites.

AURKA enhances SDCBP stability through regulation of its phosphorylation

We then investigated the consequence of the interaction between AURKA and SDCBP. Western blotting results showed that AURKA knockdown resulted in a reduction in the protein expression of SDCBP (Fig. 4a). However, we did not observe a decrease in SDCBP mRNA levels after AURKA knockdown (Fig. 4b), indicating that AURKA regulated SDCBP expression at the posttranscriptional level. To explore the underlying mechanism, we checked the effect of AURKA knockdown on SDCBP protein stability. As shown in Fig. 4c, AURKA depletion accelerated CHX-induced SDCBP protein degradation. In light of the high levels of AURKA in ESCC, we wanted to further explore the effect of AURKA overexpression on SDCBP expression and stability. The results showed that forced expression of AURKA increased SDCBP protein expression but not the mRNA level (Fig. 4d, e). Furthermore, AURKA overexpression slowed CHX-induced SDCBP degradation (Fig. 4f).

To elucidate whether SDCBP protein degradation occurs through the proteasome-mediated ubiquitylation pathway, ESCC cells were treated with CHX, with or without MG132, a proteasome inhibitor. As shown, MG132 rescued CHX-induced SDCBP protein degradation, which suggested that the stability of the SDCBP protein was regulated by a proteasome-mediated pathway (Fig. S3). Furthermore, AURKA depletion reduced SDCBP expression, whereas treatment with MG132 rescued SDCBP expression levels (Fig. 4g). Finally, to investigate whether AURKA regulated SDCBP degradation through an ubiquitylation mechanism, we detected ubiquitinated SDCBP in AURKA knockdown cells. As expected, the immunoprecipitation results indicated that knockdown of AURKA led to increased ubiquitylation of SDCBP (Fig. 4g). In contrast, elevated AURKA expression in HEK293T cells decreased SDCBP ubiquitylation (Fig. 4h), thus confirming that AURKA stabilizes SDCBP protein levels by inhibiting ubiquitination-mediated degradation.

To further investigate the importance of S131 and T200 phosphorylation on SDCBP protein stability, we generated phosphorylation-deficient mutants of the two sites. The data revealed that single mutants of S131 and T200 showed limited effects on SDCBP stability and ubiquitination (Fig. S4a–c). Then, we generated the phosphorylation-deficient double mutant (denoted as 2A) and phosphorylation-mimetic double mutant (denoted as 2D) to investigate whether the two sites work together to affect SDCBP stability. The data showed that after CHX treatment, SDCBP-2A stability dramatically decreased compared with that of the SDCBP-WT, whereas SDCBP-2D restored its stability (Fig. 4i, j). Consistent with these data, there was a notable reduction in SDCBP-2A protein expression, but not SDCBP-2D protein expression, compared with that of the SDCBP-WT, and MG132 rescued SDCBP-2A protein expression (Fig. 4k, m). Finally, we sought to demonstrate whether phosphorylation at S131 and T200 directly affected SDCBP ubiquitination. In both HEK293T and KYSE410 cells, more ubiquitin bound to SDCBP-2A than to SDCBP-WT and SDCBP-2D cells (Fig. 4l, m). Taken together, these data highlight the roles of phosphorylation at S131 and T200 sites in SDCBP protein stability and ubiquitination.

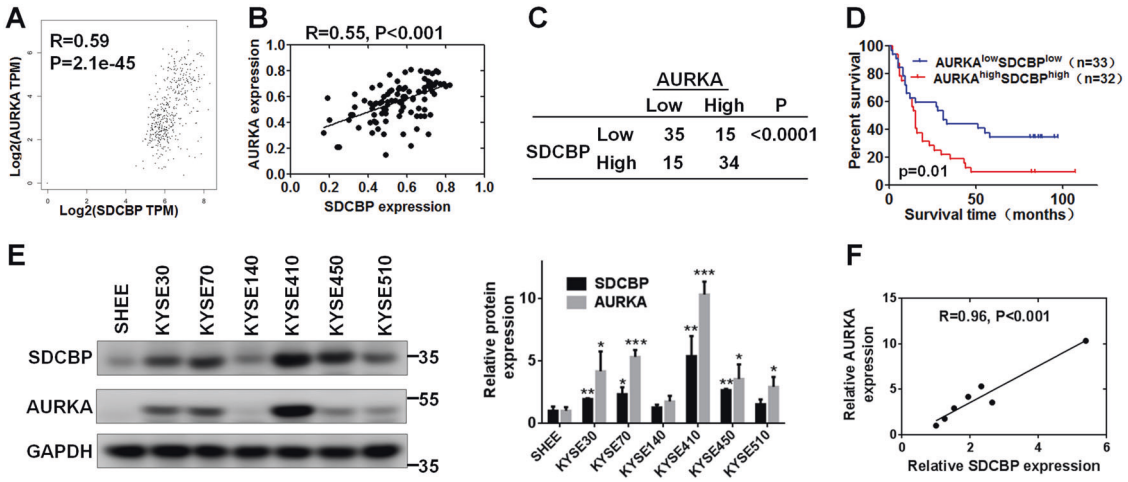

Fig. 2 Upregulated SDCBP correlates with AURKA expression in ESCC. a The correlation between SDCBP and AURKA expression based on data derived from GEPIA. **b** The correlation between SDCBP and AURKA expression levels in the ESCC tissue microarray. **c** A summary of tissue microarray results of the number of patients based on AURKA expression in $SDCBP^{low}$ and $SDCBP^{high}$ cases. **d** Relationship between patients with $SDCBP^{low}AURKA^{low}$ expression, $SDCBP^{high}AURKA^{high}$ expression and overall survival in the ESCC tissue microarray. **e** Western blotting (left panel) and quantification (right panel) of SDCBP and AURKA expression in six human ESCC cell lines and the normal esophageal epithelial cell line SHEE. Protein expression was normalized to GAPDH. **f** The correlation between SDCBP and AURKA expression levels in ESCC cell lines and SHEE cell. Statistical analysis was performed using Spearman's nonparametric correlation test in (**b**, **f**); Student's unpaired *t* test in (**e**); Fisher's exact test in (**c**); Kaplan–Meier analysis in (**d**). $*P < 0.05$, $**P < 0.01$, $***P < 0.001$. Error bars represent the mean ± SD.

SDCBP promotes ESCC proliferation in vitro and in vivo

Aberrant cell proliferation is a hallmark of cancer, and elimination of uncontrolled cell proliferation is favorable in cancer therapy [31, 32]. To examine whether SDCBP can affect ESCC proliferation, two different shSDCBP sequences were designed to establish SDCBP knockdown KYSE410, KYSE450, and KYSE70 cells, and the protein abundance of SDCBP was greatly decreased in shSDCBP cells compared with control cells (Fig. 5a). Next, we used MTT and soft agar colony formation assays to assess whether SDCBP had effects on cell proliferation and colony formation in ESCC. Our results indicated that knockdown of SDCBP slowed cell growth and lead to the formation of fewer colonies in KYSE410, KYSE450, and KYSE70 cells compared to control cells (Figs. 5b, c and S5a). To further confirm the oncogenic function of SDCBP, pcDNA3.1-3×Flag-SDCBP was transfected into KYSE30 and KYSE510 cells. The overexpression efficiency was assessed by Western blotting analysis, and the results showed that the SDCBP was successfully overexpressed in KYSE30 and KYSE510 cells (Fig. 5d). As expected, overexpression of SDCBP significantly promoted cell growth and colony formation in KYSE30 and KYSE510 cells compared to control cells (Fig. 5e, f). To evaluate the role of SDCBP on tumor growth in vivo, we established tumor xenografts in SCID mice. The results revealed that SDCBP knockdown tremendously slowed xenografted tumor growth (Fig. 5g, h), and the tumor weight also decreased significantly (Fig. 5i). These results indicated that SDCBP is an important promoter of ESCC proliferation in vitro and in vivo.

To further investigate whether SDCBP is a functional downstream factor of AURKA, a rescue assay was performed. KYSE410 cells infected with scramble or shAURKA virus were transfected with vector or Flag-SDCBP plasmid, respectively (Fig. S5b). As indicated, AURKA inhibition notably decreased cell proliferation and colony formation, whereas SDCBP partially rescued cell survival inhibition after AURKA depletion (Fig. S5c–e).

SDCBP regulates EGFR signaling by binding with EGFR and affecting EGFR internalization

An earlier study indicates the colocalization and interaction of SDCBP with EGFR in urothelial cell carcinoma [22]. Similar to this report, our results also showed that endogenous SDCBP interacted with endogenous EGFR in KYSE410 cells (Fig. 6a). Interestingly, EGFR also immunoprecipitated AURKA, which suggested that SDCBP, AURKA, and EGFR may form a protein complex (Fig. 6a). Furthermore, in HEK293T cells transfected with both SDCBP and EGFR plasmids, exogenously expressed SDCBP and EGFR pulled down each other (Fig. 6b). We then attempted to further investigate which domain of SDCBP can bind with EGFR, and the results indicated that the PDZ2 domain of SDCBP can directly bind with EGFR

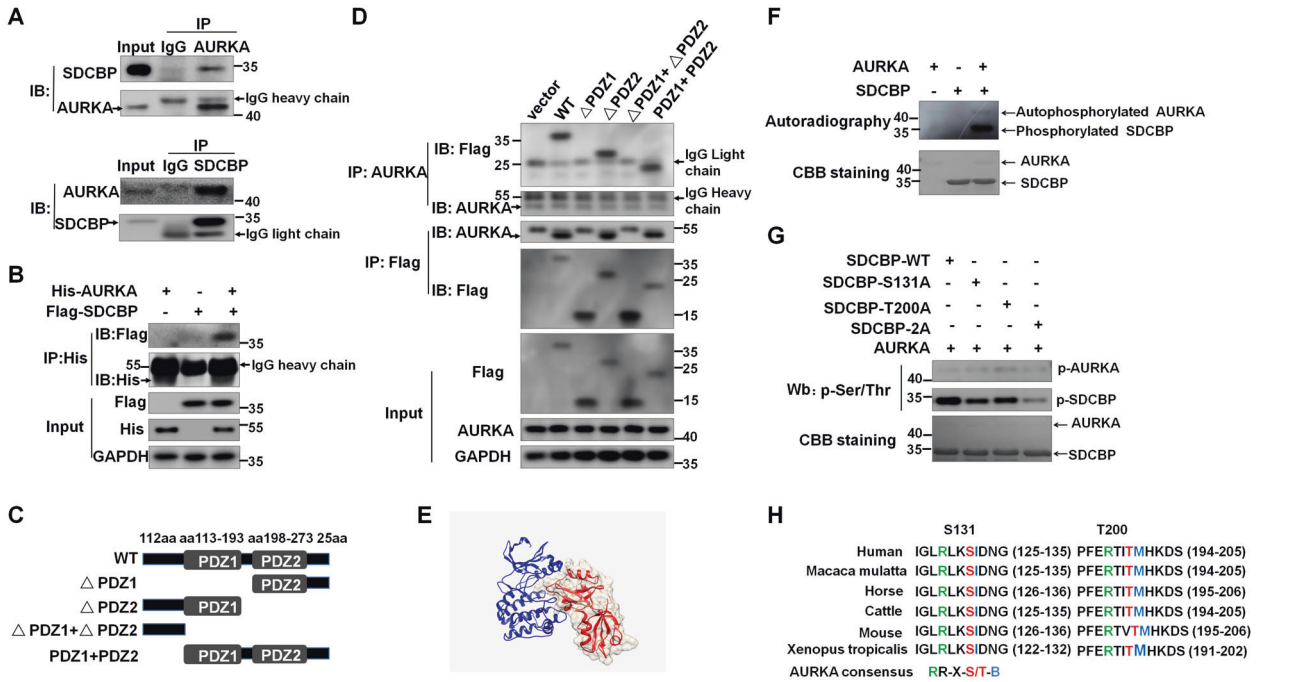

Fig. 3 SDCBP interacts with AURKA and is phosphorylated by AURKA. a Lysates from KYSE410 cells were immunoprecipitated with anti-AURKA or anti-SDCBP and then immunoblotted with the indicated antibodies. **b** His-tagged AURKA and Flag-tagged SDCBP plasmids were transiently transfected into HEK293T cells, His-tagged AURKA was immunoprecipitated by anti-His, and Flag-tagged SDCBP was detected by Western blotting. **c** Illustration of different SDCBP PDZ domain deletion constructs. **d** 293T cells were transfected with the indicated Flag-tagged SDCBP deletion mutants. Cell lysates were immunoprecipitated with anti-AURKA or anti-Flag and then analyzed by Western blotting. **e** Modeling of SDCBP binding with AURKA. AURKA is colored blue, and SDCBP is colored red with 70% transparency. **f** An in vitro kinase assay was performed in the presence of [γ-^{32}P] ATP, and the phosphorylation signal was visualized by autoradiography. **g** Recombined SDCBP-WT and SDCBP-S131A, SDCBP-T200A, and SDCBP-2A were incubated with active AURKA following an in vitro kinase assay. Phosphorylation signals were determined by Western blotting. **h** Sequence alignment of the AURKA phosphorylation consensus within SDCBP orthologs from different species. Phosphorylated serine or threonine residues are highlighted in red, arginine at the $n-3$ position is highlighted in green, and hydrophobic residues at the $n+1$ position are highlighted in blue.

(Fig. 6c). To determine whether SDCBP is involved in the EGFR signaling pathway, Western blotting was performed. The results showed that knockdown of SDCBP downregulated p-EGFR (Tyr845), p-EGFR (Tyr1068) and p-EGFR (Tyr1086), which represent EGFR activity or the EGFR autophosphorylation signal, respectively (Fig. 6d). The attenuated p-EGFR (Tyr1068) signal was also observed after SDCBP knockdown in the immunofluorescence assay (Fig. S6). As the PI3K/Akt-mediated signaling pathway is a major downstream pathway of EGFR, we observed that phosphorylated Akt^{Ser473} and PI3K^{Tyr467} levels also decreased after SDCBP knockdown (Fig. 6d).

Many studies have reported that EGFR internalization by endocytosis results in EGFR signal attenuation. To further investigate how EGFR signaling was regulated by SDCBP, alteration of EGFR membrane localization was evaluated following SDCBP knockdown. Immunocytofluorescence confocal microscopy showed that a more clustered pattern of internalized EGFR was observed in SDCBP knockdown cells compared with control cells (Fig. 6e, f). These observations were supported by fluorescence-activated cell sorting analysis, which showed a significantly lower intensity of membrane EGFR when SDCBP was depleted (Fig. 6g, h). This result suggested that SDCBP might prevent the internalization of EGFR from the cell membrane into the cytoplasm.

Phosphorylation of SDCBP by AURKA sustains SDCBP oncogenic function through EGFR signaling

Given the critical role of S131 and T200 phosphorylation in controlling SDCBP stability, we continued to investigate whether phosphorylation was involved in the oncogenic function of SDCBP in ESCC. As SDCBP-2A overexpression resulted in significant SDCBP protein degradation, to gain equivalent SDCBP protein expression, we used six-well plates to transfect different amounts of SDCBP-WT and SDCBP-2D and compared SDCBP expression with SDCBP-2A. Western blotting results showed that 1.5 μg SDCBP-WT, 1.5 μg SDCBP-2D, and 2 μg SDCBP-2A demonstrated similar SDCBP expression levels, and we used this amount of plasmid for subsequent experiments (Figs. S7a and 7a). The results showed that SDCBP-2A

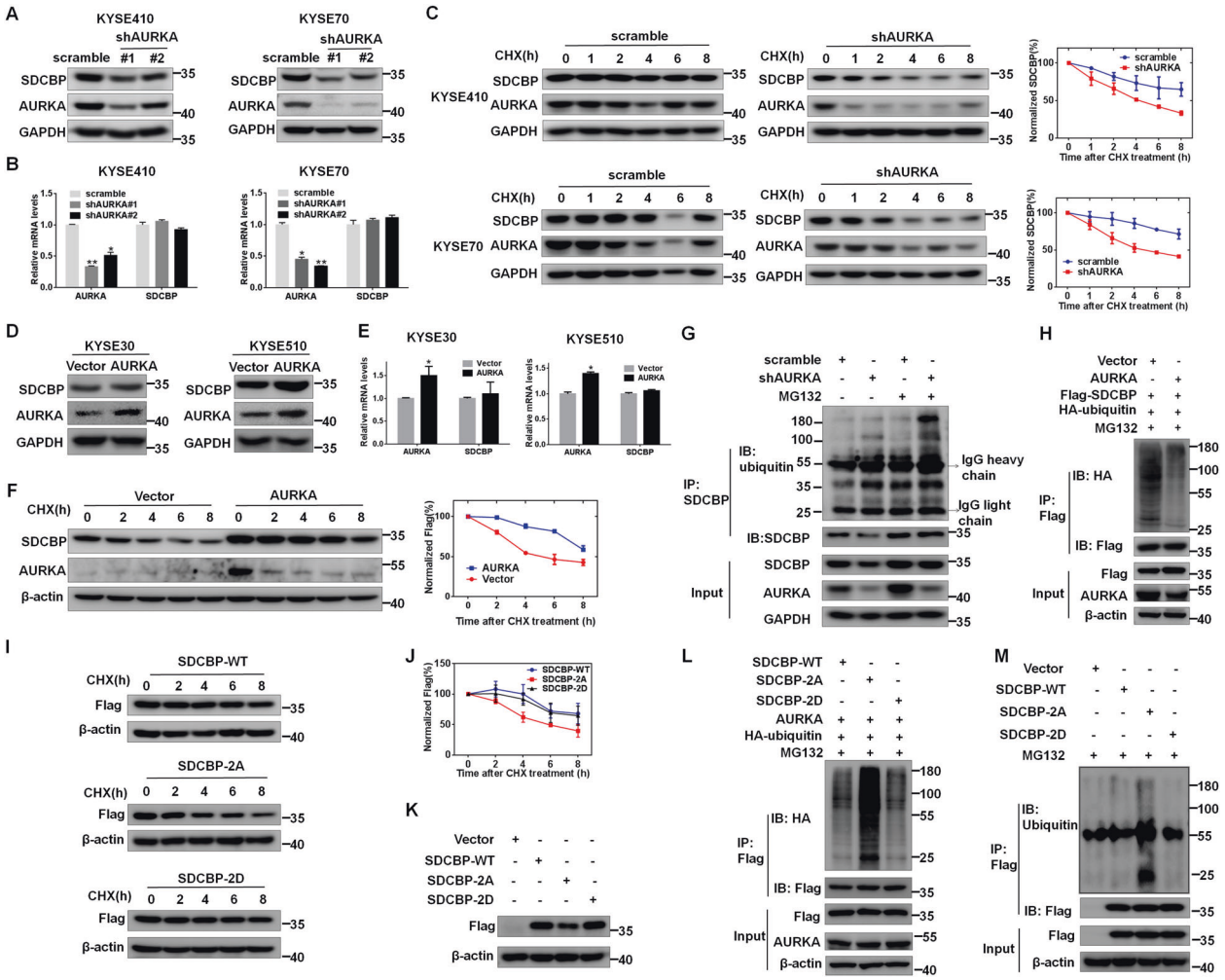

Fig. 4 AURKA enhances SDCBP stability through regulation of its phosphorylation. ESCC cells were stably infected with lentiviral scramble, shAURKA#1 or shAURKA#2, followed by immunoblotting to detect AURKA and SDCBP protein expression (**a**), and RT-PCR to detect AURKA and SDCBP mRNA expression (**b**). **c** Left panel: cells stably infected with lentiviral scramble or shAURKA were treated with 50 μg/mL CHX for the indicated time points and cell lysates were immunoblotted with specific antibodies. Right panel: quantification of SDCBP expression normalized to GAPDH expression. KYSE30 and KYSE510 cells were transfected with empty vector or pcDNA4.0-AURKA. The expression of AURKA and SDCBP was detected by Western blotting (**d**) and RT-PCR (**e**). **f** HEK293T cells were transfected with empty vector or pcDNA4.0-AURKA together with Flag-SDCBP. After 36 h of transfection, cells were treated with 50 μg/mL CHX for the indicated time points and cell lysates were immunoblotted with specific antibodies. Quantification of SDCBP expression is shown in the right panel. **g** KYSE410 cells stably infected with lentiviral scramble or shAURKA#1 were treated with or without 20 μM MG132 for 6 h and then subjected to immunoprecipitation and Western blotting analysis with the indicated antibodies. **h** HEK293T cells were transfected with the indicated constructs. Cell lysates were then subjected to immunoprecipitation and Western blotting analysis with the indicated antibodies. **i** Flag-tagged SDCBP-WT, SDCBP-2A and SDCBP-2D were transfected into KYSE410 cells and treated with 50 μg/mL CHX for different times. The expression levels of SDCBP were determined by Western blotting. **j** Quantification of SDCBP expression normalized to β-actin expression is shown. **k** Flag-tagged SDCBP-WT, SDCBP-2A, and SDCBP-2D were transfected into KYSE410 cells, and SDCBP expression was determined. HEK293T cells (**l**) and KYSE410 cells (**m**) were transfected with the indicated constructs. The samples were then subjected to immunoprecipitation and Western blotting analysis with the indicated antibodies. Unpaired Student's *t* test was used in (**b, e**). $^{*}P < 0.05$, $^{**}P < 0.01$. Error bars represent the mean ± SD from three independent experiments.

displayed much lower proliferation potential than SDCBP-WT and SDCBP-2D in the MTT assay and colony formation assay (Figs. 7b, c and S7b). In an anchorage-dependent growth assay, SDCBP-2A cells formed fewer and smaller colonies than SDCBP-WT cells. Furthermore, SDCBP-2D cells could rescue the decreased colony formation ability by SDCBP-2A cells (Fig. 7d). These data suggest that phosphorylation of SDCBP at S131 and T200 sites is critical for its oncogenic function.

Subsequently, we further investigated whether the downstream signaling pathway is affected by the phosphorylation of SDCBP. Western blotting results indicated

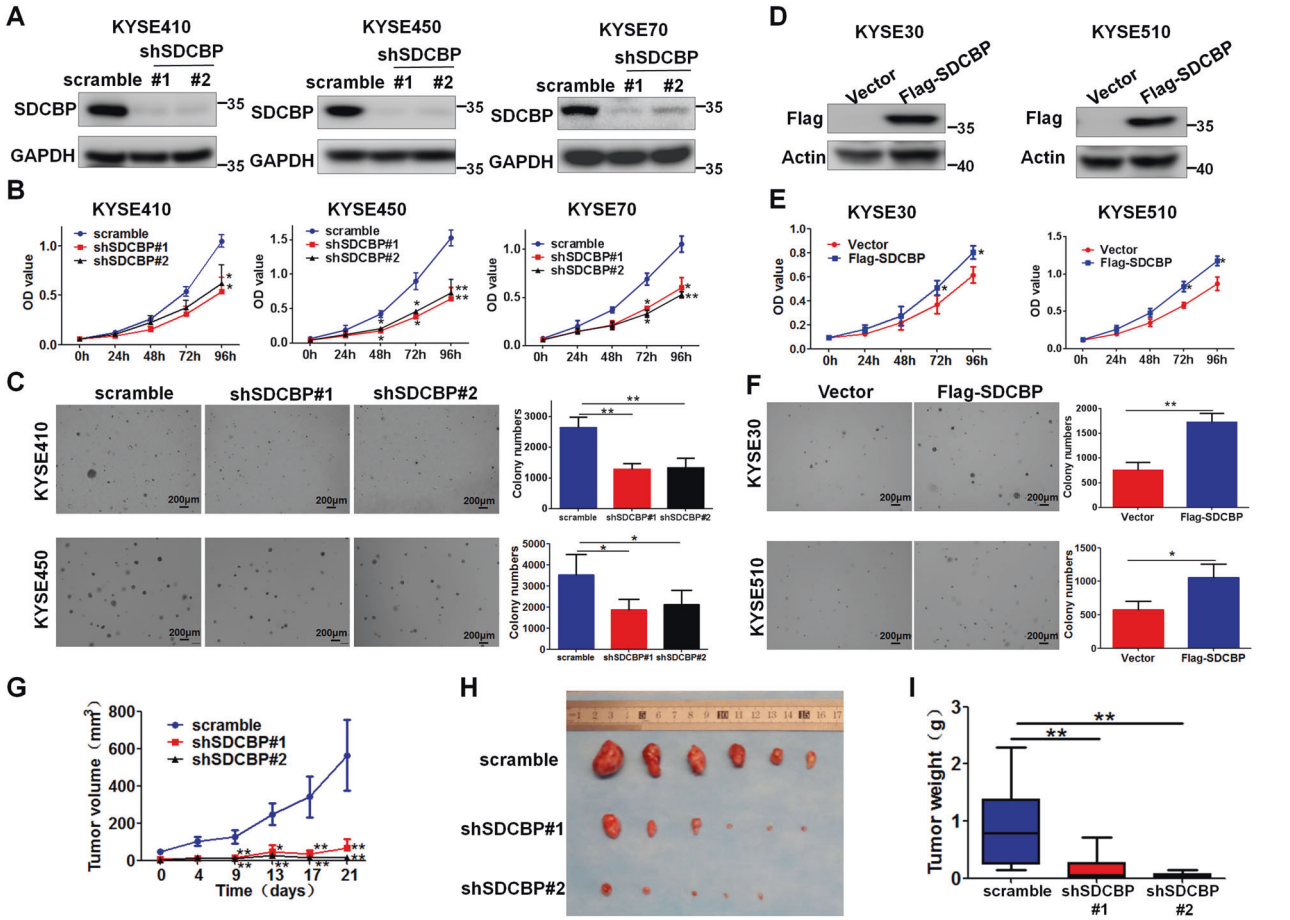

Fig. 5 SDCBP promotes ESCC cell growth in vitro and in vivo. a Endogenous SDCBP was efficiently decreased by shRNA targeting SDCBP in KYSE410, KYSE450 and KYSE70 cells. The knockdown efficiency of SDCBP was detected by Western blotting. Cell proliferation was measured upon SDCBP knockdown by MTT (**b**) and soft agar colony formation (**c**) assays. **d** KYSE30 and KYSE510 cells were transiently transfected with Flag empty vector and Flag-SDCBP. The overexpression efficiency of SDCBP was detected by Western blotting. Cell proliferation was measured upon SDCBP overexpression by MTT (**e**) and soft agar colony formation (**f**) assays. **g** KYSE450 cells stably infected with lentiviral scramble or shSDCBP were subcutaneously injected into the right flank of each mouse. When tumors were palpable after 1 month, tumor sizes were monitored every 4–5 days. **h** Tumors were excised from SCID mice at the end of the experiment. Photographs of tumors from each group are shown. **i** Tumor weight was measured after tumors were excised. Unpaired Student's *t* test was used in (**b**, **c**) (right panel), (**e**, **f**) (right panel), (**g**, **i**). $*P < 0.05$, $**P < 0.01$. Error bars represent the mean ± SD from four independent experiments for the in vitro cell experiments.

that SDCBP-2A cells resulted in decreased signal of EGFR autophosphorylation and EGFR downstream p-Akt (Ser473) and p-PI3K (Tyr467) signals compared with those in SDCBP-WT cells; however, SDCBP-2D cells can reactivate these signals (Figs. 7e and S7c). SDCBP is an adapter protein that drives tumor progression by interacting with its partners. In KYSE410 cells, endogenous SDCBP had a direct interaction with EGFR, FAK, and c-Src by immunoprecipitation assay (Fig. S7d). Results showed that SDCBP-2A cells showed reduced binding ability with EGFR, FAK, and c-Src compared with SDCBP-WT and SDCBP-2D cells (Fig. 7f). Finally, we investigated whether SDCBP phosphorylation can affect EGFR membrane localization. The immunofluorescence results indicated that EGFR was mainly located in the cell membrane in SDCBP-WT and SDCBP-2D cells but homogeneously expressed in SDCBP-2A cells (Fig. 7g, h). Consistently, EGFR membrane expression intensity was further measured by flow cytometry, and the results showed that membrane EGFR intensity in SDCBP-2A cells was significantly lower than that in SDCBP-WT and SDCBP-2D cells (Fig. 7i, j). Collectively, these findings reveal that SDCBP phosphorylation by AURKA alters EGFR membrane localization, thus affecting EGFR signal transduction.

Lentivirus-mediated SDCBP knockdown inhibits tumor growth of patient-derived xenografts in ESCC

To further determine the effect of SDCBP on ESCC progression in vivo, a patient-derived xenograft (PDX) model

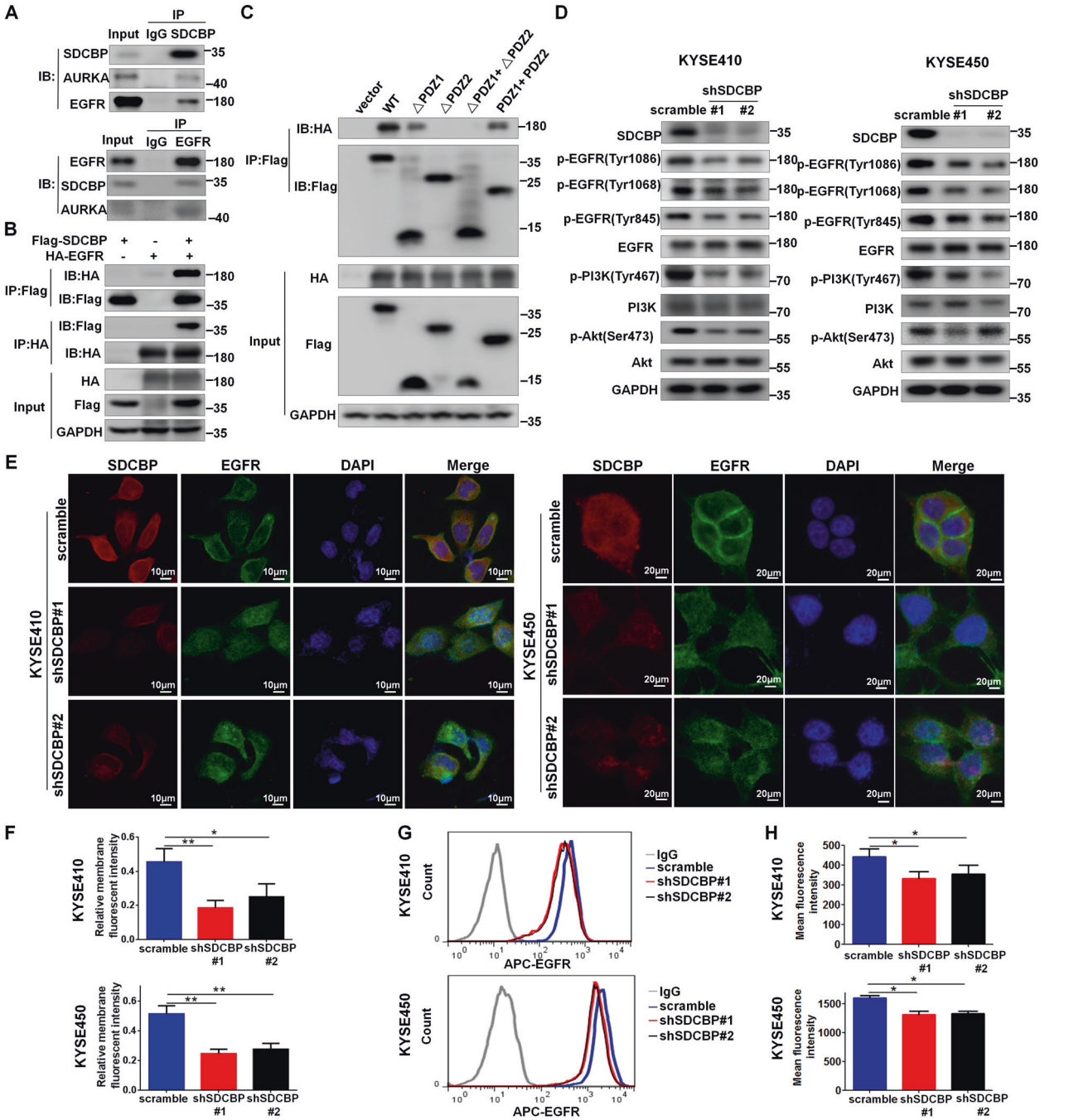

Fig. 6 SDCBP regulates EGFR signaling through binding with EGFR and affecting EGFR membrane localization. a Lysates from KYSE410 cells were immunoprecipitated with anti-EGFR or anti-SDCBP and then immunoblotted with the indicated antibodies. **b** The HA-tagged EGFR and Flag-tagged SDCBP plasmids were transiently transfected into HEK293T cells. The samples were then subjected to immunoprecipitation and Western blotting analysis with the indicated antibodies. **c** HEK293T cells were transfected with the indicated SDCBP deletion mutants and HA-tagged EGFR, and cell lysates were immunoprecipitated with anti-Flag and then analyzed by Western blotting using antibodies as indicated. **d** Cell lysates from KYSE410 and KYSE450 control cells and SDCBP knockdown cells were immunoblotted with the indicated antibodies. **e** Immunofluorescence assays were performed using the indicated cells. The localizations of EGFR and SDCBP were detected by confocal laser scanning microscopy as indicated, and the fluorescent intensity of membrane EGFR compared to the total EGFR was quantified in (**f**). **g** The expression levels of EGFR on the membrane of KYSE410 and KYSE450 cells infected with the indicated virus were measured using flow cytometry, and the curves represented the mean fluorescence intensity. **h** The mean fluorescence intensity in (**g**) was statistically analyzed. Unpaired Student's *t* test was used in (**f**, **h**). $^{*}P < 0.05$, $^{**}P < 0.01$. Error bars represent the mean ± SD from five independent experiments.

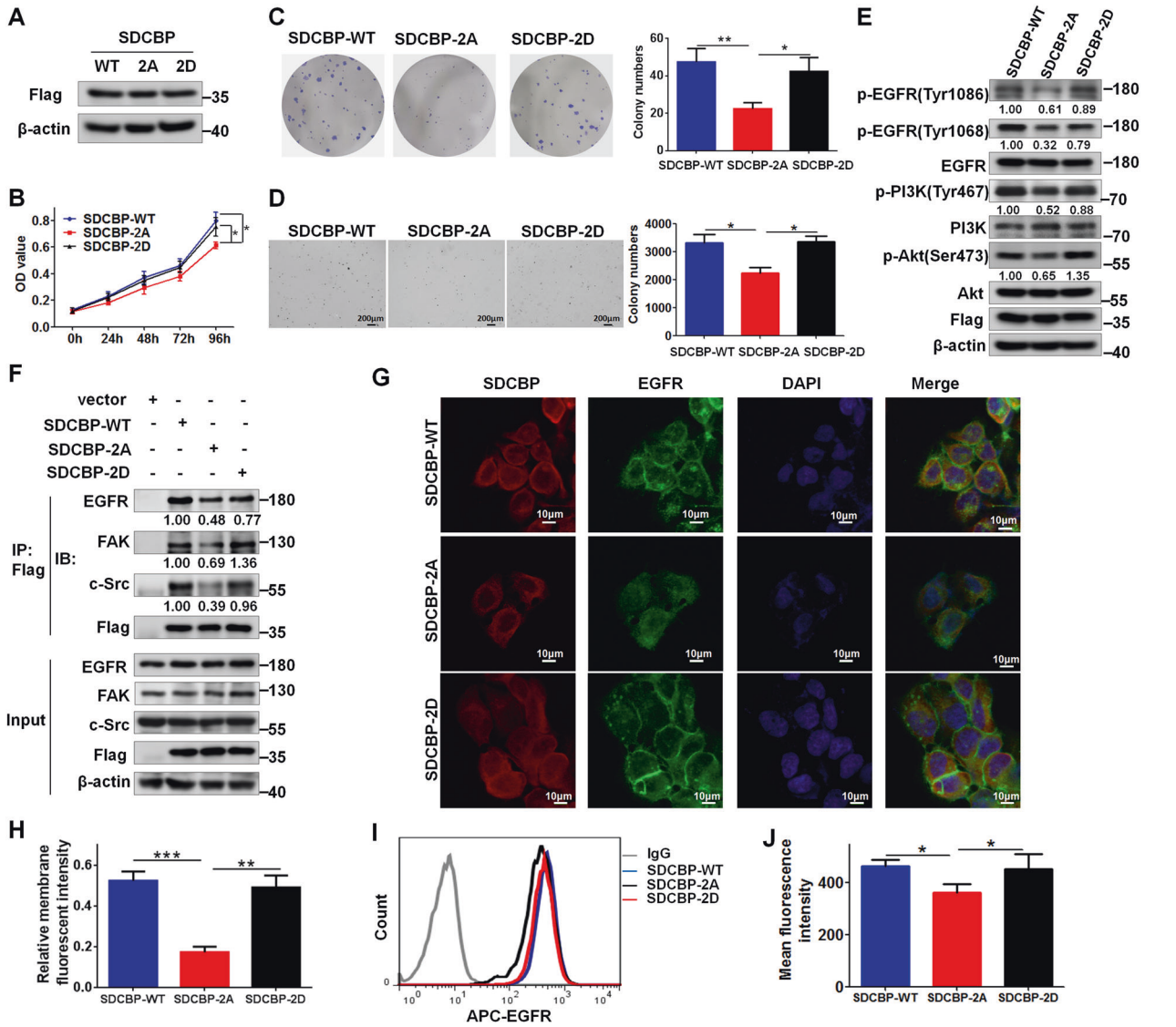

Fig. 7 Phosphorylation of SDCBP by AURKA sustains SDCBP oncogenic function through EGFR signaling. a Flag-tagged SDCBP-WT, SDCBP-2A and SDCBP-2D were transfected into KYSE410 cells, and the expression levels of Flag-SDCBP were detected. Cell proliferation was measured by MTT (**b**) and plate colony formation (**c**) assays. **d** A soft agar colony formation assay was also performed for the indicated cells. **e** Cell lysates from SDCBP-WT, SDCBP-2A and SDCBP-2D cells were immunoblotted with the indicated antibodies. **f** Flag-tagged SDCBP-WT, SDCBP-2A and SDCBP-2D were transfected into KYSE410 cells, cell lysates were subjected to immunoprecipitation and Western blotting analysis with the indicated antibodies. **g** Immunofluorescence assays were performed using SDCBP-WT, SDCBP-2A and SDCBP-2D cells. The localization of EGFR and SDCBP was detected by confocal laser scanning microscopy. **h** Quantification of the fluorescence intensity of membrane EGFR compared to that of total EGFR. **i** Cell surface expression levels of EGFR in the indicated cells were determined using flow cytometry, and the mean fluorescence intensity was analyzed in (**j**). Unpaired Student's *t* test was used in (**b**), (**c**) (right panel), (**d**) (right panel), and (**j**). $^{*}P < 0.05$, $^{**}P < 0.01$, $^{***}P < 0.001$. Error bars represent the mean ± SD from four independent experiments.

was used, and lentivirus-mediated treatment was performed. We measured SDCBP expression in different ESCC tissues and we found the case LEG92 had high expression of SDCBP (Fig. 8a). Therefore, we chose LEG92 to conduct virus infection. The results showed that SDCBP knockdown by lentivirus markedly reduced ESCC PDX tumor volume and average tumor weight compared with those of the control group (Fig. 8b–d). Next, to further check whether the antitumor effect was associated with its inhibition of EGFR signaling, tumor extracts from each group were prepared and analyzed for the expression levels of SDCBP, Ki67, p-PI3K (Tyr467), and p-Akt (Ser473). Immunohistochemistry analysis results showed that the SDCBP expression was reduced by lentiviral infection and that the expression of the cell proliferation marker Ki67 expression decreased (Fig. 8e, f). Furthermore, EGFR downstream signals p-PI3K (Tyr467) and p-Akt (Ser473) were reduced in the

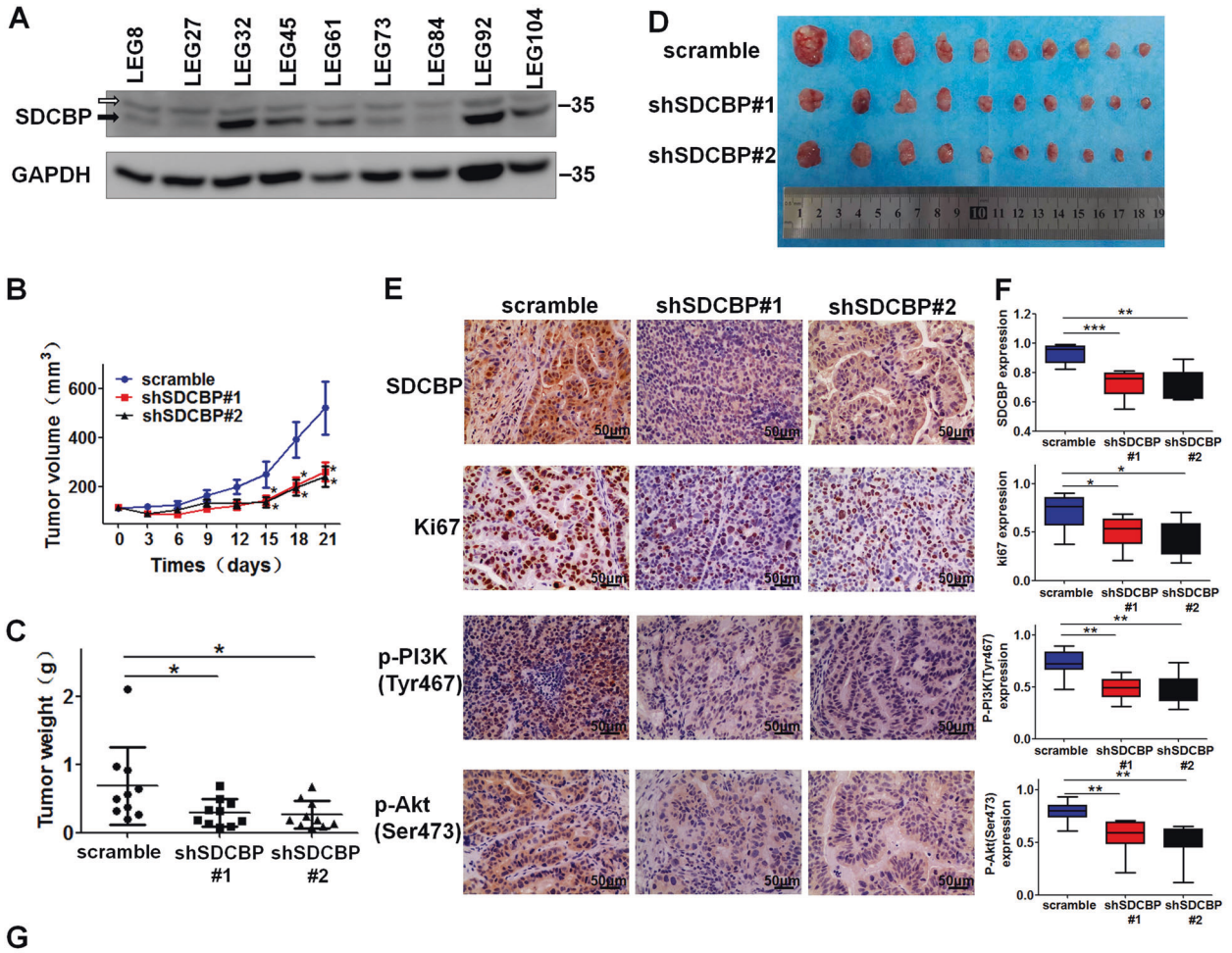

SDCBP inhibition group compared with that in the control group (Fig. 8e, f). Overall, these data provide strong evidence that inhibition of SDCBP suppresses PDX tumor growth in ESCC in vivo.

Discussion

We reported here for the first time that SDCBP showed upregulated expression in ESCC tissues as well as ESCC

◀ **Fig. 8 Lentivirus-mediated SDCBP knockdown inhibits ESCC tumor growth of patient-derived xenografts. a** SDCBP expression from tumor tissues of ESCC patients was measured by Western blotting analysis. Black arrow: SDCBP; White arrow: GAPDH. **b** Tumor sizes were monitored every three days for three continuous weeks. **c** Tumor weight was measured at the end of the experiment. **d** Tumor images from the indicated groups were shown. **e** SDCBP, Ki67, p-PI3K (Tyr467), and p-Akt (Ser473) expression in harvested xenograft tissues were assessed by immunohistochemistry. Representative photographs for each antibody in different groups were shown. **f** The statistical analysis for the immunohistochemistry images was shown. **g** A schematic model of the findings of this paper: Aberrant AURKA in ESCC binds with SDCBP and phosphorylates SDCBP at S131 and T200 sites, maintaining SDCBP stability by inhibiting ubiquitination. The accumulated SDCBP activates the EGFR-PI3K-Akt signaling pathway and finally promotes ESCC tumor growth. Unpaired Student's *t* test was used in (**b**, **c**, **f**). $*P < 0.05$, $**P < 0.01$, $***P < 0.001$. Error bars represent the mean ± SD.

cell lines compared with adjacent tissues or normal esophageal epithelial cells. Increased SDCBP expression in ESCC tissues distinguished patients in more advanced clinical stages and predicted poor survival. The underlying mechanisms for increased SDCBP expression in cancer include gene amplification, promoter hypomethylation, gene mutation, microRNA regulation, posttranscriptional modification, and so on. According to the cBioPortal for Cancer Genomics (http://www.cbioportal.org/) and the COSMIC database (http://cancer.sanger.ac.uk/cosmic), there are no somatic mutations of SDCBP in ESCC. In addition, there is no genomic amplification or hypomethylation of SDCBP in other types of cancer [22, 33, 34]. These data suggest that undefined posttranscriptional mechanisms may regulate SDCBP expression and function.

Ubiquitination is an important posttranslational mechanism involved in proteasome-dependent proteolysis. Several studies have reported that AURKA can regulate protein degradation through the proteasome-mediated ubiquitylation pathway. For example, AURKA interacts with cyclin B1 and enhances its stability in ESCC [35]. In human neuroblastoma, AURKA plays an important role in regulating N-Myc protein turnover [36]. AURKA decreases survivin ubiquitylation and degradation in gastric cancer to promote drug resistance [37]. Furthermore, phosphorylation of Twist and ALDH1A1 by AURKA in pancreatic cancer increases protein stability [38, 39]. Similar to previous studies, our findings also indicated that SDCBP protein stability was maintained by AURKA through the ubiquitylation pathway. Thus, SDCBP stability was regulated by AURKA at the posttranscriptional level.

It is reported that SDCBP can bind to ubiquitin and that the conserved LYPSL sequences in SDCBP are essential for binding to ubiquitin. Ulk1-dependent phosphorylation of Ser6 in LYPSL prevents the interaction of syntenin-1 with ubiquitin [40]. As AURKA belongs to a family of serine/threonine kinases, our data indicate that SDCBP can be phosphorylated by AURKA at Ser131 and Thr200 sites and that phosphorylation by AURKA prevents SDCBP ubiquitylation, thereby maintaining SDCBP stability. Studies on proteomics have shown that phosphorylation of key regulatory proteins always occurs at multiple sites [41]. Thus, multisite phosphorylation of SDCBP may elucidate the mechanism for ubiquitin-mediated SDCBP protein degradation.

SDCBP plays a role by interacting with a variety of regulatory proteins via its specific conserved domains. Many protein ligands show a preference for the PDZ2 domain of SDCBP. It is reported that the PDZ2 domain of syntenin-1 forms a direct antiparallel interaction with the syndecan-4 cytoplasmic domain, negatively regulating the functions of syndecan-4 [42]. In the interaction with c-Src, the PDZ2 domain of SDCBP is a major binding domain, and PDZ1 acts as a complementary binding domain [25]. Although the SDCBP PDZ1 domain tends to have weaker binding properties to the target protein than the PDZ2 domain according to its structure, the merlin-derived peptide is selective for the PDZ1 domain [43]. Furthermore, the SDCBP PDZ1 domain, not the PDZ2 domain, binds with slug when regulating nuclear slug protein function [44]. Here, we show that AURKA exclusively binds with the PDZ1 domain of SDCBP instead of the PDZ2 domain, which suggests that both SDCBP PDZ domains may work differentially and independently in various contexts.

Earlier studies showed that SDCBP mediated the upregulation of cellular proliferation via EGFR signaling in urothelial cell carcinoma [22]. Furthermore, SDCBP maintains protective autophagy through the phosphorylation of BCL2 and suppresses high levels of autophagy through EGFR signaling in glioma stem cells [23, 24]. Consistent with previous reports, we observed that SDCBP inhibition can decrease EGFR phosphorylation. Furthermore, the EGFR downstream signaling pathways p-PI3K and p-Akt are also suppressed after SDCBP knockdown. Studies have suggested that EGFR internalization by endocytosis results in EGFR signal attenuation. We found that SDCBP depletion accelerated EGFR translocation from the membrane to the cytoplasm, inhibiting EGFR activation.

Based on our study, we also found that SDCBP, EGFR, and AURKA can bind with each other in ESCC cells, which suggests that AURKA, SDCBP, and EGFR may form a signaling complex in ESCC. Structurally, the PDZ1 domain of SDCBP binds with AURKA, while the PDZ2 domain binds with EGFR. It is reported that increased AURKA expression in cancers causes phosphorylation and increased activity of many EGFR downstream effectors, including PI3K-Akt signaling, which contribute to increases in cell survival, migration, and chemoresistance [45–47]. Therefore, overexpressed SDCBP in ESCC may act as an adapter molecule that facilitates functional interaction between AURKA and AURKA downstream targets, amplifying oncogenic signaling.

Phosphorylation is a posttranslational modification that regulates various cellular functions, such as cell growth, differentiation, apoptosis, and cell signaling. The gain or loss of phosphorylation has been attributed to the principal mechanisms behind deregulated function and signal transduction [48]. Although SDCBP is stabilized via phosphorylation by AURKA at both sites identified, it appears that phosphorylation also affects its function independently of its protein levels. The phosphorylation-dead SDCBP mutant represses cell proliferation, transformation, and EGFR-PI3K-Akt signaling activities. Furthermore, the loss of phosphorylation at the two sites impairs the ability of SDCBP to bind with its reported partners, including EGFR, FAK, and c-Src, subsequently affecting their downstream signaling pathways. To our knowledge, this is the first study that investigates the SDCBP phosphorylation sites that control SDCBP oncogenic function.

Our present study indicates that high expression of SDCBP plays an important role in ESCC progression and predicts poor patient survival. We reveal a novel mechanism of SDCBP regulation, which is triggered by AURKA in a phosphorylation-dependent manner, as proposed in Fig. 8g. SDCBP phosphorylation by AURKA maintains its stability by inhibiting ubiquitination. Furthermore, SDCBP phosphorylation by AURKA maintains the oncogenic function of SDCBP by activating the EGFR-PI3K-Akt signaling pathway. Overall, our findings show that the AURKA–SDCBP–EGFR axis plays an important role in ESCC tumor progression and that SDCBP might be a novel therapeutic target for ESCC.

Materials and methods

Cell culture and reagents

Human ESCC cell lines (KYSE30, KYSE70, KYSE140, KYSE410, KYSE450, and KYSE510) were purchased from the Type Culture Collection of the Chinese Academy of Sciences (Shanghai, China). The human immortalized normal esophageal epithelial cell line SHEE was donated by Dr. Enmin Li from the Laboratory of Tumor Pathology (Shantou University Medical College, Shantou, Guangdong, China). The detailed information about cell culture and reagents can be found in the "Supplementary materials and methods" online.

Plasmids construction

All the plasmids bought from company or constructed by ourselves were confirmed by DNA sequencing. The detailed information was provided in "Supplementary materials and methods" online.

Western blotting analysis and immunoprecipitation

Cell extracts were subjected to Western blotting or immunoprecipitation following the detailed protocols in "Supplementary materials and methods," which are available online.

Cell proliferation assay and soft agar colony formation assay

Cell proliferation was measured using MTT assay or the plate colony formation assay. Colony formation ability of ESCC cell lines was detected by soft agar colony formation assay. For more details, please see the "Supplementary materials and methods" online.

Lentiviral construction and infection

To generate SDCBP and AURKA knockdown cells, the lentiviral expression vector pLKO.1 was used. The detailed information can be found online in the "Supplementary materials and methods."

Computational docking model

First, the three-dimensional (3D) structures of AURKA and SDCBP were derived from the Protein Data Bank [49]. The PDB entries are 2J4Z [50] for AURKA and 1OBZ [51] for SDCBP. The 3D First Fourier transform-based protein-docking algorithm of HEX 8.00 [52] was then used for docking experiments to assess the possible binding mode between AURKA and SDCBP. We selected 100 sorted docked configuration possibilities for further analysis.

Immunohistochemistry

A human ESCC tissue array and tumor tissues from the mouse experiment were subjected to immunohistochemistry assay and more details can be found online in the "Supplementary materials and methods."

Immunofluorescence

To evaluate the expression and distribution of SDCBP and EGFR, KYSE410 and KYSE450 cells were subjected to immunofluorescence assay. For more details, please see the "Supplementary materials and methods" online.

Flow cytometry

The expression intensity of EGFR at the plasma membrane was determined by flow cytometry analysis. More details can be found in the "Supplementary materials and methods."

Real-time quantitative PCR

Total RNA was extracted using TRIzol Reagent (TAKARA, Dalian, China). The primers sequences and detailed processes were in the "Supplementary materials and methods" online.

Purification of recombinant SDCBP proteins

Wild type SDCBP and different mutant expression constructs were generated by subcloning into the pet28a vector. For more details, please see the "Supplementary materials and methods" online.

In vitro kinase assay

The phosphorylation of SDCBP-WT or SDCBP site mutants by AURKA was detected by in vitro kinase assay. Detailed experimental procedures was provided in the "Supplementary materials and methods" online.

In vivo cell-derived and patient-derived xenograft mouse model

This study was approved by the Ethics Committee of Zhengzhou University (Zhengzhou, Henan, China). Detailed experimental procedures was provided in the "Supplementary materials and methods" online.

Statistical analysis

All statistical tests were two sided, and $P < 0.05$ was considered statistically significant. All statistical analysis was performed using Graph-Pad Prism 6 and SPSS 22.0 software.

Acknowledgements This study was supported by the National Natural Science Foundation of China (Nos. 81802795 and 31301144); the Key Scientific Research Project Plan of Colleges and Universities in Henan Province (No. 18A310034); the Science and Technology Project of Henan Province (Nos. 182102310324 and 202102310206); and the Training plan for Young Backbone Teachers of Zhengzhou University (No. 2018ZDGGJS037).

Compliance with ethical standards

Conflict of interest The authors declare that they have no conflict of interest.

Publisher's note Springer Nature remains neutral with regard to jurisdictional claims in published maps and institutional affiliations.

References

1. Melhado RE, Alderson D, Tucker O. The changing face of esophageal cancer. Cancers. 2010;2:1379–404.
2. Bray F, Ferlay J, Soerjomataram I, Siegel RL, Torre LA, Jemal A. Global cancer statistics 2018: GLOBOCAN estimates of incidence and mortality worldwide for 36 cancers in 185 countries. CA Cancer J Clin. 2018;68:394–424.
3. Gao YB, Chen ZL, Li JG, Hu XD, Shi XJ, Sun ZM, et al. Genetic landscape of esophageal squamous cell carcinoma. Nat Genet. 2014;46:1097–102.
4. Zeng H, Chen W, Zheng R, Zhang S, Ji JS, Zou X, et al. Changing cancer survival in China during 2003-15: a pooled analysis of 17 population-based cancer registries. Lancet Glob Health. 2018;6: e555–e67.
5. Dutertre S, Descamps S, Prigent C. On the role of aurora-A in centrosome function. Oncogene. 2002;21:6175–83.
6. Tong T, Zhong Y, Kong J, Dong L, Song Y, Fu M, et al. Overexpression of Aurora-A contributes to malignant development of human esophageal squamous cell carcinoma. Clin Cancer Res. 2004;10:7304–10.
7. Tanaka E, Hashimoto Y, Ito T, Okumura T, Kan T, Watanabe G, et al. The clinical significance of Aurora-A/STK15/BTAK expression in human esophageal squamous cell carcinoma. Clin Cancer Res. 2005;11:1827–34.
8. Yang SB, Zhou XB, Zhu HX, Quan LP, Bai JF, He J, et al. Amplification and overexpression of Aurora-A in esophageal squamous cell carcinoma. Oncol Rep. 2007;17:1083–8.
9. Wang X, Lu N, Niu B, Chen X, Xie J, Cheng N. Overexpression of Aurora-A enhances invasion and matrix metalloproteinase-2 expression in esophageal squamous cell carcinoma cells. Mol Cancer Res. 2012;10:588–96.
10. Baietti MF, Zhang Z, Mortier E, Melchior A, Degeest G, Geeraerts A, et al. Syndecan-syntenin-ALIX regulates the biogenesis of exosomes. Nat Cell Biol. 2012;14:677–85.
11. Ohno K, Koroll M, El Far O, Scholze P, Gomeza J, Betz H. The neuronal glycine transporter 2 interacts with the PDZ domain protein syntenin-1. Mol Cell Neurosci. 2004;26:518–29.
12. Zimmermann P, Tomatis D, Rosas M, Grootjans J, Leenaerts I, Degeest G, et al. Characterization of syntenin, a syndecan-binding PDZ protein, as a component of cell adhesion sites and microfilaments. Mol Biol Cell. 2001;12:339–50.
13. Sala-Valdes M, Gordon-Alonso M, Tejera E, Ibanez A, Cabrero JR, Ursa A, et al. Association of syntenin-1 with M-RIP polarizes Rac-1 activation during chemotaxis and immune interactions. J Cell Sci. 2012;125:1235–46.
14. Das SK, Bhutia SK, Kegelman TP, Peachy L, Oyesanya RA, Dasgupta S, et al. MDA-9/syntenin: a positive gatekeeper of melanoma metastasis. Front Biosci. 2012;17:1–15.
15. Boukerche H, Su ZZ, Prevot C, Sarkar D, Fisher PB. mda-9/Syntenin promotes metastasis in human melanoma cells by activating c-Src. Proc Natl Acad Sci USA. 2008;105:15914–9.
16. Boukerche H, Su ZZ, Emdad L, Baril P, Balme B, Thomas L, et al. mda-9/Syntenin: a positive regulator of melanoma metastasis. Cancer Res. 2005;65:10901–11.
17. Koo TH, Lee JJ, Kim EM, Kim KW, Kim HD, Lee JH. Syntenin is overexpressed and promotes cell migration in metastatic human breast and gastric cancer cell lines. Oncogene. 2002;21:4080–8.
18. Qian XL, Li YQ, Yu B, Gu F, Liu FF, Li WD, et al. Syndecan binding protein (SDCBP) is overexpressed in estrogen receptor negative breast cancers, and is a potential promoter for tumor proliferation. PLoS One. 2013;8:e60046.
19. Zhong D, Ran JH, Tang WY, Zhang XD, Tan Y, Chen GJ, et al. Mda-9/syntenin promotes human brain glioma migration through focal adhesion kinase (FAK)-JNK and FAK-AKT signaling. Asian Pac J Cancer Prev. 2012;13:2897–901.
20. Kegelman TP, Das SK, Hu B, Bacolod MD, Fuller CE, Menezes ME, et al. MDA-9/syntenin is a key regulator of glioma pathogenesis. Neuro Oncol. 2014;16:50–61.

21. Cui L, Cheng S, Liu X, Messadi D, Yang Y, Hu S. Syntenin-1 is a promoter and prognostic marker of head and neck squamous cell carcinoma invasion and metastasis. Oncotarget 2016;7:82634–47.
22. Dasgupta S, Menezes ME, Das SK, Emdad L, Janjic A, Bhatia S, et al. Novel role of MDA-9/syntenin in regulating urothelial cell proliferation by modulating EGFR signaling. Clin Cancer Res. 2013;19:4621–33.
23. Talukdar S, Pradhan AK, Bhoopathi P, Shen XN, August LA, Windle JJ, et al. MDA-9/Syntenin regulates protective autophagy in anoikis-resistant glioma stem cells. Proc Natl Acad Sci USA. 2018;115:5768–73.
24. Yoshida GJ. Molecular machinery underlying the autophagic regulation by MDA-9/Syntenin leading to anoikis resistance of tumor cells. Proc Natl Acad Sci USA. 2018;115:E7652–E3.
25. Boukerche H, Aissaoui H, Prevost C, Hirbec H, Das SK, Su ZZ, et al. Src kinase activation is mandatory for MDA-9/syntenin-mediated activation of nuclear factor-kappaB. Oncogene. 2010;29:3054–66.
26. Luyten A, Mortier E, Van Campenhout C, Taelman V, Degeest G, Wuytens G, et al. The postsynaptic density 95/disc-large/zona occludens protein syntenin directly interacts with frizzled 7 and supports noncanonical Wnt signaling. Mol Biol Cell. 2008;19:1594–604.
27. Egea-Jimenez AL, Gallardo R, Garcia-Pino A, Ivarsson Y, Wawrzyniak AM, Kashyap R, et al. Frizzled 7 and PIP2 binding by syntenin PDZ2 domain supports Frizzled 7 trafficking and signalling. Nat Commun. 2016;7:12101.
28. Kegelman TP, Wu B, Das SK, Talukdar S, Beckta JM, Hu B, et al. Inhibition of radiation-induced glioblastoma invasion by genetic and pharmacological targeting of MDA-9/Syntenin. Proc Natl Acad Sci USA. 2017;114:370–5.
29. Liu J, Qu J, Zhou W, Huang Y, Jia L, Huang X, et al. Syntenin-targeted peptide blocker inhibits progression of cancer cells. Eur J Med Chem. 2018;154:354–66.
30. Ferrari S, Marin O, Pagano MA, Meggio F, Hess D, El-Shemerly M, et al. Aurora-A site specificity: a study with synthetic peptide substrates. Biochem J. 2005;390:293–302.
31. Lopez-Saez JF, de la Torre C, Pincheira J, Gimenez-Martin G. Cell proliferation and cancer. Histol Histopathol. 1998;13:1197–214.
32. Mori H, Sugie S, Yoshimi N, Hara A, Tanaka T. Control of cell proliferation in cancer prevention. Mutat Res. 1999;428:291–8.
33. Gangemi R, Mirisola V, Barisione G, Fabbi M, Brizzolara A, Lanza F, et al. Mda-9/syntenin is expressed in uveal melanoma and correlates with metastatic progression. PLoS ONE. 2012;7:e29989.
34. Oyesanya RA, Bhatia S, Menezes ME, Dumur CI, Singh KP, Bae S, et al. MDA-9/Syntenin regulates differentiation and angiogenesis programs in head and neck squamous cell carcinoma. Oncoscience. 2014;1:725–37.
35. Qin L, Tong T, Song Y, Xue L, Fan F, Zhan Q. Aurora-A interacts with Cyclin B1 and enhances its stability. Cancer Lett. 2009;275:77–85.
36. Otto T, Horn S, Brockmann M, Eilers U, Schuttrumpf L, Popov N, et al. Stabilization of N-Myc is a critical function of Aurora A in human neuroblastoma. Cancer Cell. 2009;15:67–78.
37. Kamran M, Long ZJ, Xu D, Lv SS, Liu B, Wang CL, et al. Aurora kinase A regulates Survivin stability through targeting FBXL7 in gastric cancer drug resistance and prognosis. Oncogenesis. 2017;6:e298.
38. Wang J, Nikhil K, Viccaro K, Chang L, Jacobsen M, Sandusky G, et al. The Aurora-A-Twist1 axis promotes highly aggressive phenotypes in pancreatic carcinoma. J Cell Sci. 2017;130:1078–93.
39. Wang J, Nikhil K, Viccaro K, Chang L, White J, Shah K. Phosphorylation-dependent regulation of ALDH1A1 by Aurora kinase A: insights on their synergistic relationship in pancreatic cancer. BMC Biol. 2017;15:10.
40. Rajesh S, Bago R, Odintsova E, Muratov G, Baldwin G, Sridhar P, et al. Binding to syntenin-1 protein defines a new mode of ubiquitin-based interactions regulated by phosphorylation. J Biol Chem. 2011;286:39606–14.
41. Humphrey SJ, James DE, Mann M. Protein phosphorylation: a major switch mechanism for metabolic regulation. Trends Endocrinol Metab. 2015;26:676–87.
42. Choi Y, Yun JH, Yoo J, Lee I, Kim H, Son HN, et al. New structural insight of C-terminal region of Syntenin-1, enhancing the molecular dimerization and inhibitory function related on Syndecan-4 signaling. Sci Rep. 2016;6:36818.
43. Kang BS, Cooper DR, Jelen F, Devedjiev Y, Derewenda U, Dauter Z, et al. PDZ tandem of human syntenin: crystal structure and functional properties. Structure. 2003;11:459–68.
44. Wang LK, Pan SH, Chang YL, Hung PF, Kao SH, Wang WL, et al. MDA-9/Syntenin-Slug transcriptional complex promote epithelial-mesenchymal transition and invasion/metastasis in lung adenocarcinoma. Oncotarget. 2016;7:386–401.
45. Yao JE, Yan M, Guan Z, Pan CB, Xia LP, Li CX, et al. Aurora-A down-regulates IkappaBalpha via Akt activation and interacts with insulin-like growth factor-1 induced phosphatidylinositol 3-kinase pathway for cancer cell survival. Mol Cancer. 2009;8:95.
46. Guan Z, Wang XR, Zhu XF, Huang XF, Xu J, Wang LH, et al. Aurora-A, a negative prognostic marker, increases migration and decreases radiosensitivity in cancer cells. Cancer Res. 2007;67:10436–44.
47. Yang H, He L, Kruk P, Nicosia SV, Cheng JQ. Aurora-A induces cell survival and chemoresistance by activation of Akt through a p53-dependent manner in ovarian cancer cells. Int J Cancer. 2006;119:2304–12.
48. Radivojac P, Baenziger PH, Kann MG, Mort ME, Hahn MW, Mooney SD. Gain and loss of phosphorylation sites in human cancer. Bioinformatics. 2008;24:i241–7.
49. Berman HM, Westbrook J, Feng Z, Gilliland G, Bhat TN, Weissig H, et al. The protein data bank. Nucleic acids Res. 2000;28:235–42.
50. Fancelli D, Moll J, Varasi M, Bravo R, Artico R, Berta D, et al. 1,4,5,6-tetrahydropyrrolo[3,4-c]pyrazoles: identification of a potent Aurora kinase inhibitor with a favorable antitumor kinase inhibition profile. J Med Chem. 2006;49:7247–51.
51. Kang BS, Cooper DR, Devedjiev Y, Derewenda U, Derewenda ZS. Molecular roots of degenerate specificity in syntenin's PDZ2 domain: reassessment of the PDZ recognition paradigm. Structure. 2003;11:845–53.
52. Macindoe G, Mavridis L, Venkatraman V, Devignes MD, Ritchie DW. HexServer: an FFT-based protein docking server powered by graphics processors. Nucleic Acids Res. 2010;38:W445–9.